AN IMPROVED METHOD FOR CALCULATING PROTON LINAC CAVITIES

M. Martini , D.J. Warner

European Organization for Nuclear Research
Geneva , Switzerland

Introduction

An improved method for calculating the electromagnetic fields in a linac cavity of Alvarez type is presented.

The solution of a finite difference form of the wave equation is obtained by the combined use of analytical formulae and the point successive over-relaxation (SOR) technique.

By limiting the application of the numerical approach to the axial region of the linac cell where the complicated shape of boundary renders it unavoidable and in using analytical expansions elsewhere, an improved precision is obtained in a relatively short computer time. This precision is tested by comparison of our results with those of other authors and by computing for each case a "normalization factor" which proves to be a sensitive check parameter.

A Fortran program, CLAS (Cern Linear Accelerator Structures), capable of treating cavities with rotational symmetry and a general drift-tube profile, was written by the authors.

A detailed account of the theory of the method used and the main features of the CLAS program can be found in Ref. [1]. Here a shorter account together with some recent results, will be given.

The Electromagnetic Problem

The rotational and image symmetries of a typical linac cell (Fig. 1) allow one to restrict study to the reduced region of Fig. 2 and to obtain a complete field solution using a convenient form of the wave equation [1]:

$$\frac{\delta^2 U}{\delta r^2} + \frac{\delta^2 U}{\delta z^2} - \frac{1}{r}\frac{\delta U}{\delta r} + k^2 U = 0 \qquad (1)$$

with the potential $U = rH\varphi$ and $k = \omega\sqrt{\mu\epsilon}$. Eq. (1) holds everywhere inside the domain ABCD whereas along the boundary the condition :

$$\frac{\delta U}{\delta n} = 0 \qquad (2)$$

applies and on the axis CD :

$$U = 0 \, . \qquad (3)$$

This in an eigenvalue problem since in Eq. (1) k^2 is not known "a priori". The required accelerating mode TM_{010} is given by the lowest eigenvalue k and corresponding eigenfunction U.

The equation for k is obtained by a variational method [1] :

$$k^2 = \min \left\{ \frac{-\iint_{ABCD} \frac{1}{r}\left[\left(\frac{\delta U}{\delta r}\right)^2 + \left(\frac{\delta U}{\delta z}\right)^2\right] dr\, dz}{\iint_{ABCD} -\frac{U^2}{r}\, dr\, dz} \right\} . \qquad (4)$$

Values of k^2 thus periodically calculated during the computation cycle converge downwards towards the correct value.

As shown later, in this method one divides the field ABCD into two regions EFCD and ABFE with an artificially introduced boundary line EF of Dirichelet type. The SOR technique is actually applied to the domain EFCD where Eq. (1) is to be solved with the boundary conditions :

i) Eq. (2) along ED and FC,
ii) Eq. (3) along DC,
iii) the artificial boundary condition :

$$U(r,z) = g(r,z) \qquad (5)$$

along EF, where $g(r,z)$ is defined later.

In the upper region ABEF an analytical expansion is used yielding a precise solution of (1) with the boundary conditions (5) along EF and (2) elsewhere.

The Finite Difference Equations

To obtain a finite difference form of Eq. (1), a net of horizontal and vertical straight lines is superimposed on the integration field ABCD. The rectilinear boundaries CD, DA, AB, BC and EF fall on mesh lines.

By using Taylor's expansions expressions of the derivatives of U appearing in Eq. (1) can be found which involve values of U only at five points. Eq. (1) can then be written for each regular internal node of the net with h , h' and the numeration U_i defined in Fig. 3.

$$U_0\left(2 + 2\frac{h^2}{h'^2}\right) - U_1 - U_3 - U_2\left(1 - \frac{h'}{2r}\right)\frac{h^2}{h'^2}$$

$$- U_4\left(1 + \frac{h'}{2r}\right)\frac{h^2}{h'^2} - k^2h^2U_0 = 0 \qquad (6)$$

where a term tending to zero like h^4 or h'^4, as $h,h' \to 0$, has been dropped.

The Irregular Points

The case of one missing neighbour

Eq. (6) cannot be applied directly to a point U_0 when one of the four neighbours lies outside the domain of integration. Then the following special procedure applies to the general case of a curved boundary crossing the mesh at some distance ξh ($0 \leq \xi \leq 1$) from U_0 (Fig. 4).

If one expresses U_1 as a function of U_0, U_2, U_3 and U_4, then one can proceed thereafter as for regular internal nodes.

At A :

$$\left(\frac{\delta U}{\delta n}\right)_A = 0 \quad \text{and} \quad \left(\frac{\delta^2 U}{\delta n\, \delta l}\right)_A = 0 \qquad (7)$$

because the boundary condition (2) is satisfied both in A and nearby along the metallic boundary. Application of Eqs.(7) and some rather cumbersome algebra [1], lead to an equation for U_1 :

$$c_1U_1 = c_2U_2 + c_3U_3 + c_4U_4 + c_5U_0 \qquad (8)$$

with

$$c_1 = \frac{1 - m^2}{1 + m^2}\left[\frac{1}{\xi}\frac{1}{2m}(1 + 2\xi) + \frac{m}{1 + m^2}\right] + \frac{h}{2R\sqrt{1 + m^2}}(1 + 2\xi)\left(m + \frac{1}{m}\right)$$

$$c_2 = \frac{m^2 - 1}{1 + m^2}\left[\frac{1}{2\xi}\frac{h}{h'} + \frac{m}{1 + m^2}\frac{h^2}{h'^2}\right] \qquad (9)$$

$$c_3 = \frac{1 - m^2}{1 + m^2}\left[\frac{1}{\xi}\frac{1}{2m}(1 - 2\xi) - \frac{m}{1 + m^2}\right] + \frac{h}{2R\sqrt{1 + m^2}}(1 - 2\xi)\left(m + \frac{1}{m}\right)$$

$$c_4 = \frac{1 - m^2}{1 + m^2}\left[\frac{1}{2\xi}\frac{h}{h'} + \frac{m}{1 + m^2}\frac{h^2}{h'^2}\right]$$

$$c_5 = \frac{1 - m^2}{1 + m^2}\left[\frac{2}{m} + \frac{2m}{1 + m^2}\left(1 - \frac{h^2}{h'^2}\right)\right] + \frac{2h\xi}{R\sqrt{1 + m^2}}\left(m + \frac{1}{m}\right)$$

where $m = \tan\alpha$ and R is the radius of curvature of the boundary profile at A.

By substituting Eqs. (8) and (9) into (6) one then obtains an equation for U_0 which neglects a term $O(h^3)$ [1]. Therefore, compared to Eq. (6), the precision obtained is one order of magnitude in h lower, and is probably the best precision achievable for such a boundary point.

The limiting cases shown in Figs. 5 and 6 can be easily deduced from Eqs. (8) and (9). When $U_1(U_3)$ falls on ED (the rectilinear part of FC) one assumes $U_1 = U_3$ in Eq. (6).

The case of two missing neighbours

For the general situation in which two neighbours are missing (Fig. 7) the boundary condition (2) is used to give :

$$U_0' = U_0 + O(h^2). \qquad (10)$$

Expressing U_0' as a linear function of U_3 and U_2 :

$$U_0 \simeq U_0' = \frac{U_3h'\cos\alpha + U_2h\sin\alpha}{h'\cos\alpha + h\sin\alpha}. \qquad (11)$$

The error expected is of the order of h^2 so that two orders of magnitude of h have been lost with respect to Eq. (6). However, since this kind of point represents, in general, only a small percentage of the irregular points, one expects, at most, some local perturbations of the final map of potentials.

The Double Iterative Process

Eventually, using Eqs. (6) to (11) one obtains an inhomogeneous linear system of N_s equations in N_s unknown U values corresponding to the much reduced number of nodes belonging to EFCD. Since the values of the function $g(r,z)$ and of k^2 are periodically redetermined during the computation cycle, one is led to solve a double iterative process, each "outer" iteration consisting of the solution of the system of N_s inhomogeneous equations :

$$n = 1,2,3\ldots \qquad \left\{B - k^{2[n-1]}h^2I\right\}[U]^{[n]} = A\,[U]^{[n]} = [g]^{[n-1]} \qquad (12)$$

where B and A are $N_s \times N_s$ matrices, I is the identity matrix, $[U]^{[n]}$ and $[g]^{[n-1]}$ are vectors of order N_s evaluated at the n-th (n - 1 th) iteration. $[g]$ is a very sparse vector giving rise to the inhomogeneity of the system and having non zero entries corresponding only to the NC nodes belonging to the Dirichelet boundary EF where NC is the number of columns of the mesh. A manner of evaluating $[g]^{[n]}$ from $[U]^{[n]}$ is given in the section on initial filling.

The entries of $[U]^{[o]}$ and $[g]^{[o]}$ correspond to the starting solution.

The solution of the system (12) required for each outer iteration, must, due to the large size of matrix, be obtained by a numerical process. As the matrix is also sparse a relaxation method is best suited. In CLAS the SOR technique is used.

The SOR Technique

It can be proved [2] that the SOR method converges and an optimum value β_o of the over-relaxation factor β, can be found, if matrix A of Eq. (12) fulfils the following requirements :

a) It has all $a_{ii} > 0$, $1 \leq i \leq N_s$, and all

$$a_{ij} \leq 0 \quad , \quad 1 \leq i \leq N_s \quad , \quad i \neq j \ .$$

b) It has property A of Young and the ordering is consistent.

c) It is irreducibly diagonally dominant.

d) It can be made symmetric by a similarity transformation of the type :

$$A_s = H^{-1} A H \qquad (13)$$

where H is a diagonal matrix.

These four properties are fully explained elsewhere [1]. Note that conditions a), c) and d) are sufficient to ensure the convergence of the method for any $0 \leq \beta \leq 2$, whilst condition b), which refers to some topological properties of the matrix A and to the order of scanning the net, must be added if one wants to employ Young's formula for optimum β :

$$\beta_o = 2 \left[1 + (1 - \bar{\mu}^2)^{1/2}\right]^{-1} \qquad (14)$$

where $\bar{\mu}$ is the dominant eigenvalue of the Jacobi matrix associated to the A matrix [1].

Considering Eq. (6) and the corresponding ones for irregular points one finds that :

i) by using the "five point" formula and by scanning the mesh from left to right and from bottom to top, the matrix A of the system (12) fulfils conditions a) and b).

ii) condition c) is only satisfied for regular internal points, if one neglects a term of the order of 10^{-5} compared with other terms of the order of unity. For the coefficients of irregular points, (9), the dependence on the particular boundary profile and mesh size, prevents any useful "a priori" generalization. Therefore the program tests the irregular points for diagonal dominance (within the same precision as for the regular points) before starting relaxation. If condition c) fails somewhere, the entries of the A matrix are recalculated with a slightly different mesh size, and the test is repeated. A satisfactory grid is usually found in two or three attempts.
This test has proved to be an important one as, by selecting only diagonally dominant matrices, a diverging case was never observed.

iii) Finally it can be proved that the part of matrix A which refers to regular internal nodes and to points lying on straight boundaries, can be made symmetric by using a similarity transformation of the type (13). Unfortunately this does not hold for the "irregular part" of A so that one eventually obtains an "approximately" symmetric matrix, that is with asymmetry in $\simeq 1$ % of the total number of entries [1].

Nevertheless, experience indicates that formula (14) yields values of β_o giving a good convergence, which compare favourably with values obtained, using trial and error methods. Moreover to the authors' knowledge there exists no alternative theory to evaluate β_o for non symmetric matrices.

The Initial Filling and The Computation Cycle

The initial filling used consists of analytical solutions originally developed for the determination of k in corrugated circular wave-guides [4]. When this method is applied to the conventional proton accelerator geometry one approximates the practical cavity by one with a right cylindrical drift-tube completely containing the actual smooth one, see Fig. 2.

Starting solutions for points between the fictive and the practical drift-tube are obtained by :

a) making the potential fall exponentially with distance inside the bore hole,

and

b) making linear extrapolations from the last two analytical values in the row elsewhere.

The formulae used for the initial filling are given in [1].

As a preliminary to the computation cycle consider the rectangular domain above the line r = a in Fig. 2. Given the values of the potential function U at the nodes of the line r = a as a Dirichelet boundary condition and the Neumann condition (2) on the metallic boundary, the following analytical expansion satisfies the wave equation (1) :

$$U(r,z) = A_o(r) + \sum_1^{\infty} A_m(r) \cos\left(\frac{m\,2\pi z}{L}\right) \qquad (15)$$

$$0 \leq z \leq \frac{L}{2}$$

$$a \leq r \leq b$$

with:

$$A_o(r) = \frac{r}{a}\,\frac{F_1(kr)}{F_1(ka)}\,A_o(a) \qquad (16)$$

$$A_m(r) = \frac{r}{a}\,\frac{G_1(\gamma_m r)}{G_1(\gamma_m a)}\,A_m(a)$$

and
$$\beta_m = \frac{m\,2\pi}{L} \qquad (17)$$

$$\gamma_m^2 = \beta_m^2 - k^2$$

$$F_1(kr) = J_1(kr) - \frac{I_o(kb)}{Y_o(kb)}\,Y_1(kr)$$

$$G_1(\gamma_m r) = I_1(\gamma_m r) - \frac{I_o(\gamma_m b)}{K_o(\gamma_m b)}\,K_1(\gamma_m r)\ .$$

To find the value of $A_m(r)$, given discrete values of $U(a,z)$, one solves :

$$U(a,z) = A_o(a) + \sum_1^{m_1} A_m(a)\,\cos\left(m\frac{2\pi z}{L}\right) \qquad (18)$$

$$\text{with}\quad 0 \leqslant z \leqslant \frac{L}{2}$$

$$m_1 < NC,$$

The following computation cycle is executed :

a) The cavity, after the initial filling, is divided into two regions by a boundary line EF located at $r = r_D$ where the initial range of variation of U with z is less than 5 % or at 2a whenever (at high energy) this condition cannot be achieved. Region I in Fig. 2 ($0 < r < r_D$), is henceforth referred to as the 'small cell'. The initial U values along EF form the constant Dirichelet boundary for the small cell.

b) Twelve iteration cycles ("inner" iterations) are done in the latter using the SOR technique.

c) A new value of k is determined from Eq. (4) by numerical integration over the whole cell using the most recent values of potentials, U, be they obtained by relaxation ($0<r<r_D$) or analytically ($r_D \leqslant r \leqslant b$). This step is explained below.

d) The coefficients $A_m(r)$ of the Fourier expansion (15) are computed from Eq. (18) and (16).

e) Using Eq. (15) and taking up to 10 harmonics, the upper part of the cell is refilled with potentials. In particular this establishes a better Dirichelet boundary along $r = r_D$.

The set of potentials for $r \geqslant r_D$ are normalized so that the potential at $r = r_D$, $z = L/4$ remains constant, i.e. to first order one makes the potentials continuous across the boundary.

Steps b), c), d) and e) constituting one "outer" iteration, are then repeated in a cyclic manner.

This overall cycle is continued, for a fixed number of iterations ($\simeq$ 100), after the frequency convergence is obtained. A few iterations ($\simeq$ 10) are then performed in the complete domain ABCD without over-relaxing (i.e. $\beta = 1$) to smooth the potential map until the stopping criterion is satisfied.

Returning to step c) consider the ideal situation when a new value of $k^2 = k^{2[n]}$ is calculated. Assuming that the numerical method has had time to completely converge, the potentials in the small cell represent a 'perfect' solution of Eq. (1) for $k^2 = k^{2[n-1]}$ satisfying appropriate boundary conditions everywhere, in particular, the inhomogeneous Dirichelet condition along $r = r_D$.

For $r_D \leqslant r \leqslant b$ the same holds true, because here the potentials have been evaluated using the analytical expansion with $k^2 = k^{2[n-1]}$. No discontinuity in U will therefore be present at $r = r_D$, but, unless both $k^{2[n-1]}$ and the Dirichelet boundary potentials correspond to the complete cavity solution, there will be a discontinuity in the axial electric field (i.e. in $\frac{\delta U}{\delta r}$) across $r = r_D$.

It is shown in [1] that Eq. (4), which is used to evaluate $k^{2[n]}$, is equivalent to :

$$k^{2[n]} = k^{2[n-1]} + \delta(k^2)^{[n-1]} \qquad (19)$$

with

$$\delta(k^2)^{[n-1]} = \frac{\int_{EF} \frac{U}{r}\,\delta\left(\frac{\delta U}{\delta r}\right)\,dz}{\iint_{ABCD} \frac{U^2}{r}\,dS} \qquad (20)$$

where $\delta\left(\frac{\delta U}{\delta r}\right)$ represents the above mentioned discontinuity of $\frac{\delta U}{\delta r}$.

It can be proved that, near resonance, the value of k^2 yielded by Eq. (19) is the best possible guess for the frequency using the set of potentials available; moreover, it can be shown that $\delta(k^2)$ is always negative and tends to zero when the U's approach the correct solution for the overall cavity ($\delta\left(\frac{\delta U}{\delta r}\right)$ tends to zero).

The Stopping Criterion and The Final Precision

The calculation is stopped at some run n when the following stopping criterion is satisfied [1]:

$$e^{[n]}_{max.} = \frac{\bar{\lambda}}{1-\bar{\lambda}} \max_{1\leq i\leq N} \left\{ U_i^{[n]} - U_i^{[n-1]} \right\} \leq \epsilon_0 U_i^{[n]} \qquad (21)$$

where $\bar{\lambda}$ is the dominant eigenvalue of the SOR matrix and $\epsilon_0 \simeq 2.5 \times 10^{-4}$. Practically by this choice of ϵ_0 the calculation is stopped before rounding off errors become imporant. Note that as the final iterations involve all the N nodes of ABCD, the search for $e^{[n]}_{max}$ must cover the same range.

The precision of the results is very difficult to evaluate. To the authors' knowledge the following is one of the most powerful tests for the 'self-consistency' of the table of potentials. Consider two methods of calculating the mean axial electric field. Two different approaches give respectively :

$$E_o = \frac{1}{2\pi f_o \epsilon L} \int_o^L \left(\frac{\delta^2 U}{\delta^2 r} \right) dz \qquad \text{at } r = 0 \qquad (22)$$

$$E'_o = \frac{2\pi f_o \mu}{L} \iint_{ABCD} \left(\frac{U}{r} \right) ds . \qquad (23)$$

With a perfectly consistent set of potentials the "normalization factor"

$$F = \frac{E_o}{E'_o} = 1 \qquad (24)$$

so the difference of F from unity indicates qualitatively the average comparative precision of the solution close to the axis and over the complete cavity.

This F factor proved to be a very sensitive check figure. For example, it was observed that using different starting solutions, mesh size and computation cycle, repeatability of frequency to better than 0.01 % was common, whereas the corresponding variation of F could be 3 %. Nevertheless by inspection of F, it is difficult to assess precisely the error expected on the potentials and on the frequency, because F is only indirectly related to values of U.

The Results

The program CLAS, which was written for the CDC 6600 and 3800 computers, allows one to calculate cavities with a general drift-tube profile.

CLAS was used to compute the resonant frequency and main electromagnetic parameters of an 18 cell 3 MeV experimental Linac [3] . The results are shown in Table I. A high average number of mesh nodes (16000 in the overall cell) was necessary to handle the fine details in the drift-tube profiles. However, since the iterations involved only $\simeq$ 2500 nodes in the small cell, the average computation time on the CDC 3800 did not exceed 20 secs. per 1000 points of the complete grid.

In Table II the results obtained for a set of cavities previously calculated by MURA MESSYMESH program are shown. It can be seen that, in general, a good agreement is achieved.

Conclusions

A compound numerical analytical approach for the calculation of electromagnetic fields in linac cavities has been described. The basic idea of employing analytical expansions in regions with simple boundary shape and matching them with solutions obtained by relaxation methods, could produce different computation cycles and be applicable to different geometries. For instance, other numerical and analytical solutions could be used and other cell partitioning and matching techniques might prove more convenient.

A thorough study of the SOR technique has stressed the importance of some properties of the A matrix. In particular the use of diagonally dominant systems of equations has always avoided divergence.

By reducing the number of coupled equations to be solved iteratively, a quicker convergence was obtained. Moreover the artificially introduced Dirichelet boundary prevented the errors, in the lower part of the cell, spreading into the outer region where a good solution was introduced. In this respect the Bessel series used gave a starting solution less complicated from a programming point of view and more flexible than that obtained extrapolating from a neighbouring cell.

Finally as the iteration time needed to scan the small cell was perhaps 10 % of the time needed for the complete cavity, many more iterations could be performed giving an accurate solution in the most useful axial region.

Acknowledgments

Thanks are due to Mr. A. Katz of Saclay from whose program and studies we have borrowed freely and to Dr. H.G. Hereward for his helpful suggestions and criticism.

References

[1] M. Martini, D.J. Warner
"Numerical Calculations of Linear Accelerator Cavities", CERN 68-11, 1968.

[2] D. Young
"Iterative Methods for Solving Partial Difference Equations of Elliptic Type", American Mathematical Society Transactions, Vol. 76, pp 92-111, 1954.

[3] M. Martini, D. J. Warner
"Improved Calculations of Proton Linac Cavities", CERN-MPS/Int. LIN 67-6, August-1967

[4] W. Walkinshaw, J.S. Bell
"A New Calculation of Slot Depth for the Metal Loaded Linear Acc." AERE T/R 864, 1952

TABLE I

Results Computed for the 3 MeV Accelerator

Cell No.	Mean Energy (MeV)	Computed Frequency (MHz)	Normalisation Factor 'F'	Transit Time Factor	Shunt Impedance MΩ/m
1	0.558	203.07	0.985	0.690	87.0
2	0.645	203.06	1.014	0.705	87.3
3	0.738	203.04	1.010	0.721	88.1
4	0.838	203.02	1.000	0.724	88.1
5	0.945	203.01	0.998	0.734	88.5
6	1.059	203.00	0.993	0.735	88.4
7	1.178	202.86	0.994	0.741	89.3
8	1.308	202.96	1.010	0.751	88.9
9	1.443	202.87	0.998	0.758	89.7
10	1.585	202.85	1.010	0.759	90.0
11	1.735	202.90	1.007	0.760	89.8
12	1.891	202.94	1.001	0.760	89.8
13	2.052	202.94	1.008	0.759	90.6
14	2.220	202.97	0.988	0.758	90.2
15	2.395	203.00	0.998	0.762	90.8
16	2.576	203.02	0.991	0.764	90.4
17	2.764	203.06	0.995	0.770	91.3
18	2.960	203.12	1.011	0.775	91.5
Mean Values		202.984 MHz	1.0006		
Standard Deviations		0.078 MHz	0.0088		

TABLE II

Comparative Table of Results of CLAS and MESSYMESH

T is the transit time factor, Z_s is the shunt impedance. PW and PDT are the power losses in the outer wall and drift-tube. E is mean cell energy. F is the normalization factor. Q is quality factor. Where applicable quantities in MKS units.

Run No.	MESSYMESH	31661	31616	20241	20242	30736	31465
	L/2	3.25	8.00	11.25	26.0	30.0	42.0
Frequency	CLAS	200.61	200.920	200.98	202.40	201.30	200.93
	MESSYMESH	201.33	201.069	201.09	202.40	201.29	200.91
E	CLAS	0.889	5.44	10.86	63.78	86.88	197.01
	MESSYMESH	0.895	5.45	10.87	63.78	86.87	196.95
T	CLAS	0.7032	0.8152	0.8173	0.7584	0.7007	0.5579
	MESSYMESH	0.6649	0.8040	0.8068	0.7484	0.6924	0.5506
PW	CLAS	577.70	1443.20	2047.73	4315.71	4993.53	6974.74
	MESSYMESH	581.52	1449.61	1985.91	4234.07	4863.45	6922.50
PDT	CLAS	407.71	738.96	1024.01	3870.88	4900.33	10161.53
	MESSYMESH	394.38	728.55	1038.76	3908.67	4988.33	10171.26
Q	CLAS	83106.2	92914.2	92953	77762.7	75418.5	65348.7
	MESSYMESH	83907.8	93249.5	93891	77945.9	75442.5	65279
Z_s	CLAS	65.96	73.32	73.25	63.52	60.64	49.02
	MESSYMESH	66.53	73.36	74.29	63.78	60.82	49.08
F	CLAS	1.008	1.001	1.006	0.998	1.002	0.998

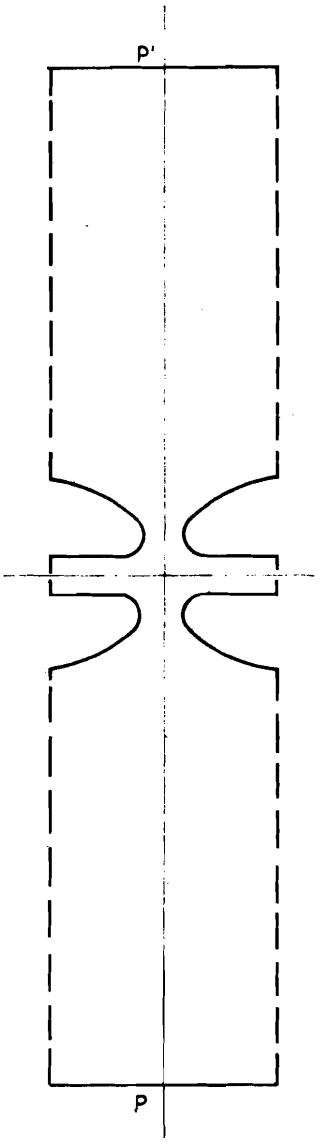

Fig. 1 Cross-section of a symmetrical accelerating cell of Alvarez type.

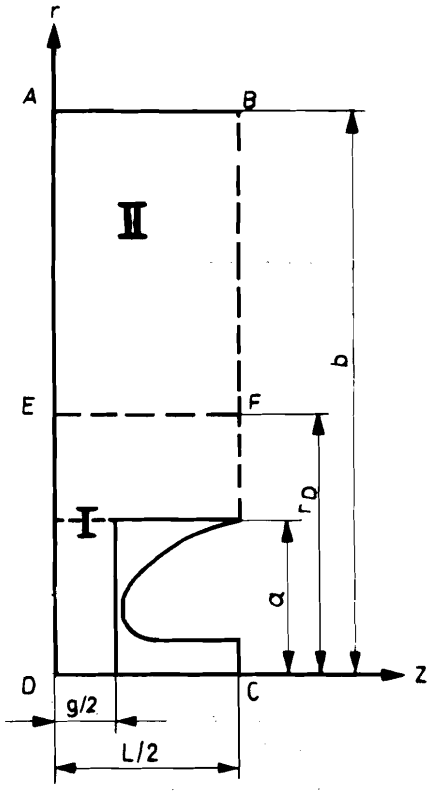

Fig. 2 Cross-section of the reduced cell showing the integration domain divided into regions I and II .

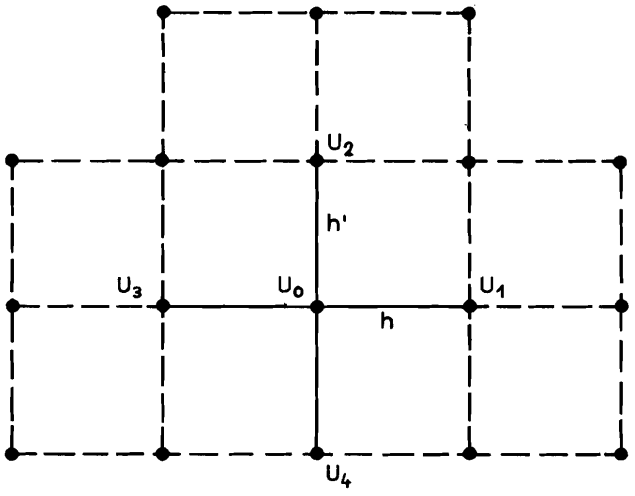

Fig. 3 Detail of grid for numerical calculations showing the potentials used in five points method.

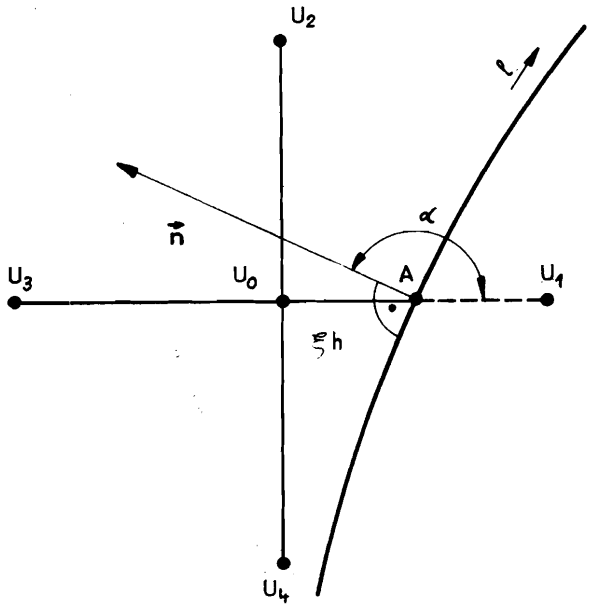

Fig. 4 Detail showing case of one missing neighbour (general boundary).

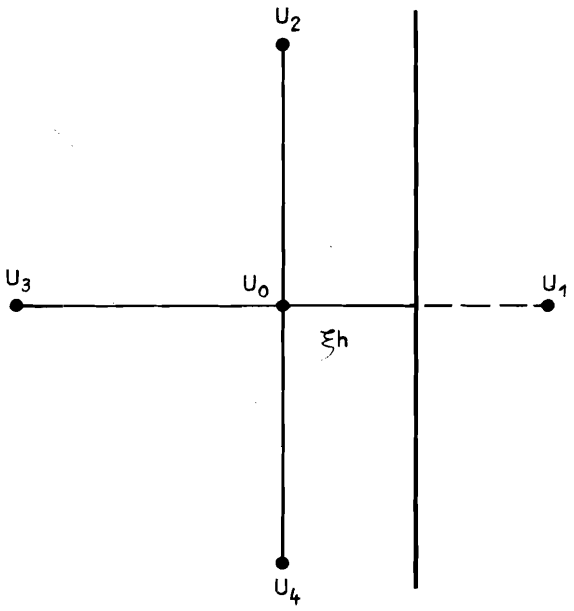

Fig. 5 As Fig. 4 but with vertical straight boundary.

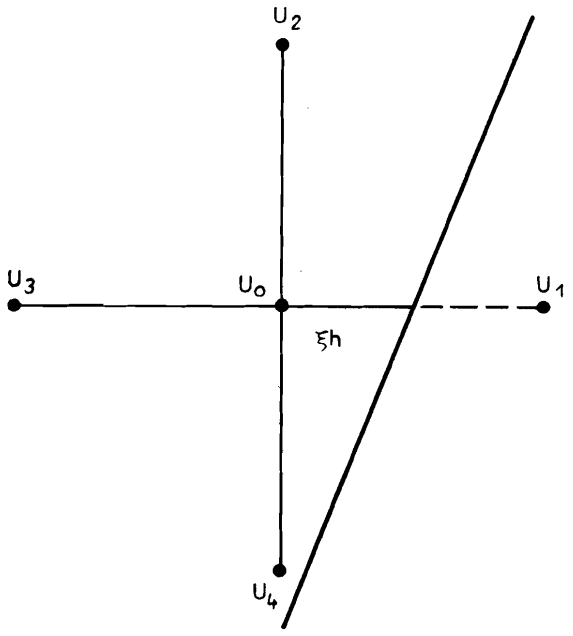

Fig. 6 As Fig. 4 but with oblique straight boundary.

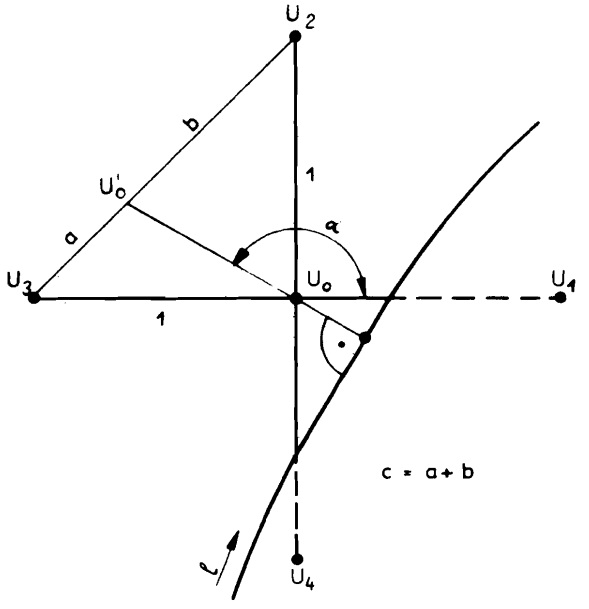

Fig. 7 Detail showing the case of two missing neighbours (general boundary).